Universidad Carlos III de Madrid
e-Archivo

Institutional Repository

This document is published in:

Powder Metallurgy (2011). 54(3), 242-252.
DOI: http://dx.doi.org/10.1179/174329009X457063

© 2011. Institute of Materials, Minerals and Mining
Published by Maney on behalf of the Institute

PM processing and characterisation of Ti–7Fe low cost titanium alloys

P. G. Esteban*, L. Bolzoni, E. M. Ruiz-Navas and E. Gordo

Department of Materials Science and Engineering, Universidad Carlos III

* Corresponding author, email pgesteba@ing.uc3m.es

Abstract: This work studies a set of low cost beta alloys with the composition Ti–7Fe, processed by conventional powder metallurgy (PM). The materials were prepared by conventional blending of elemental Ti hydride–dehydride powder with three different Fe powder additions: water atomised Fe, Fe carbonyl and master alloy Fe–25Ti. The optimal sintering behaviour and the best mechanical properties were attained with the use of Fe carbonyl powder, which reached a sintered density of up to 93% of the theoretical density, with UTS values of 800 MPa in the 'as sintered' condition. Coarse water atomised powder particles promoted reactive sintering, and coarse porosity was found due to the coalescence of Kirkendall porosity and by the pores generated during the exothermic reaction between Ti and Fe. The addition of Fe–25Ti produced brittle materials, as its low purity (91·5%) was found to be unsuitable for formulating Ti alloys.

Keywords: Titanium, Low cost alloys, Mechanical properties, Blended elemental method

Introduction

The interest in titanium alloys arises from their high specific strengths and high corrosion resistances,[1,2] properties that have been exploited by the aerospace, medical and military industries for many years. However, the main factor that hinders the use of Ti in the design of parts for most industrial applications is the high cost of the final product compared with the costs of products made of iron or steel. Nevertheless, the motor industry, and the transport industry in general, are showing interest in titanium alloys, as their use could reduce the consumption of oil and the pollution of vehicles.[3,4]

Powder metallurgy (PM) offers some advantages to Ti manufacturing with respect to overcoming the high costs of Ti products, thus encouraging researchers to study and develop Ti PM technology. These benefits are summarised as follows:

(i) powder metallurgy takes advantage of new processes designed to obtain low cost Ti. At this time, elemental Ti must be obtained by the Kroll process from rutile (TiO_2) and ilmenite ($FeTiO_3$), which is energy, labour and capital intensive. Then, Ti powders must be obtained from the metal by crushing, atomisation, the hydride–dehydride process (HDH) or the 'rotating electrode process'. This chain of processes to obtain Ti powder makes it too expensive to be processed by PM. However, many emerging techniques for the production of low cost Ti produce Ti powder directly, so PM will take direct advantage of these developments.[5] These techniques include the Armstrong process[6] and the promising electrolytic FFC-Cambridge process,[7] which is able to obtain elemental Ti in powder form or even prealloyed powder directly from TiO_2

(ii) powder metallurgy permits the scalability of manufacturing processes, which leads to cost reduction through mass production

(iii) near net shape production eliminates waste of material during manufacturing, which is especially important when processing high priced metals. Moreover, PM avoids or minimises the need for machining final parts, which is particularly interesting for Ti since it is expensive and complex to machine

(iv) temperatures achieved during the sintering process are below the melting point of the metal, which avoids or minimises the reaction and contamination of Ti with the crucibles, vessels, moulds or tooling used in other near net shape techniques (i.e. moulds in casting)

(v) powder metallurgy offers the chance to select Ti alloy compositions that are not easily processed with ingot metallurgy. One of the limitations found in ingot metallurgy is the segregation of the alloying elements during melting and solidification. Powder metallurgy permits the formation of homogeneous fine microstructures without segregation. In addition, PM allows for the manufacturing of composite materials reinforced with ceramic particles, which increases the variety of materials that are able to be processed, as well as the application field of Ti materials.

The final properties, optimum process and minimum cost must be balanced to develop a low cost alloy.

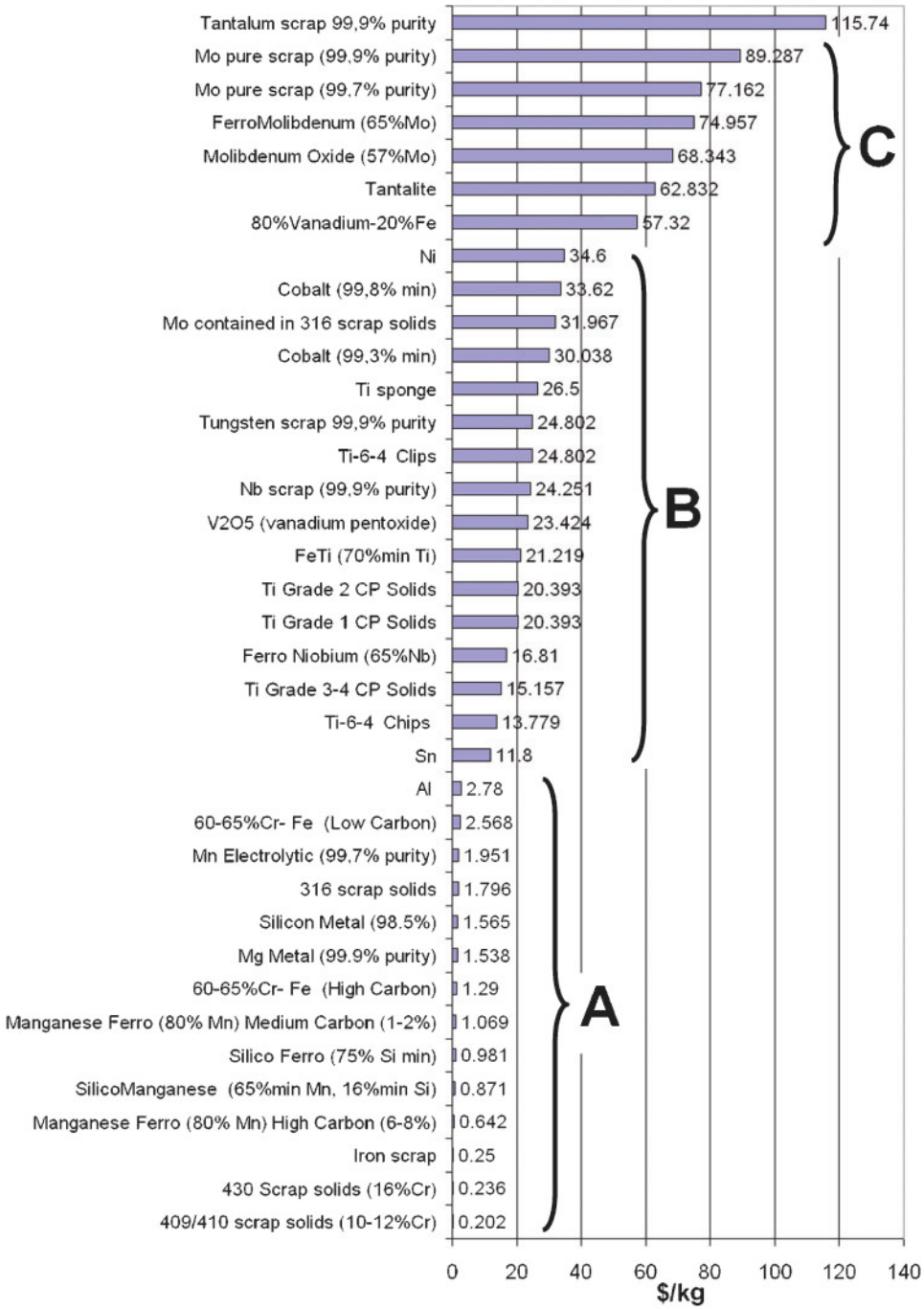

1 Prices ($/kg) of some candidate materials to be used as alloying elements for Ti (data obtained from Dow Jones and London Metals Exchange, October–November 2005)

Titanium has traditionally been developed by industries where cost has less importance than the benefits obtained from the excellent properties of the material. The final properties of low cost titanium are not supposed to be improvements on those of the aeronautic grades, but must be good enough for applicability in environments where its combination of cost and properties could offer an advantage over traditional ferrous (or non-ferrous) alloys. The success of the development of low cost titanium alloys seems to be related to selection of the right PM process (pressing + sintering), to the proper selection of the sintering conditions and to a proper choice of alloying elements.

Currently, the most employed and versatile Ti alloy is Ti–6Al–4V, which accounts for half of the production of the Ti market. Ti–6Al–4V is classified as an alpha + beta alloy, is heat treatable and attains medium strength values. The production of this alloy by PM can be carried out by means of prealloyed powders or by the use of the blending elemental approach.[8] Prealloyed powders are harder than pure Ti, and are often difficult to conventionally press. On the other hand, blended elemental powders can be a good approach to obtain parts using conventional PM techniques. Additionally, PM offers opportunities to introduce low cost alloying elements and eliminates costly vanadium from the composition, allowing for a decrease in the price of the material.

Some PM low cost Ti alloys have been designed and proposed by other researchers in recent decades.[9–14] The

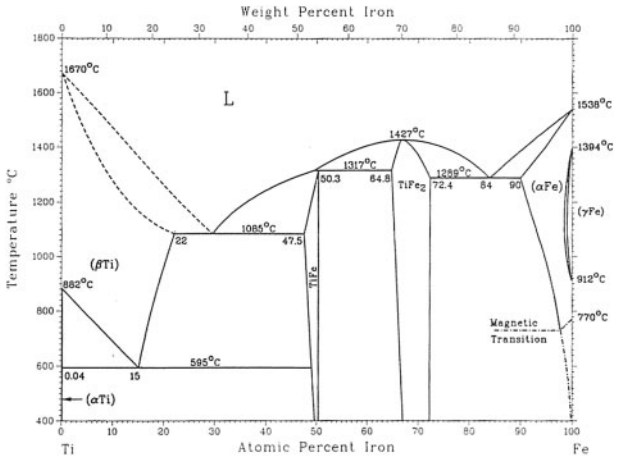

2 Equilibrium phase diagram for system Ti–Fe[16]

development of low cost alloys starts with the selection of a low cost alloying system. In Fig. 1, the prices of some materials to form alloy systems for Ti are shown, and three groups are identified in the list. These prices were obtained between October and November 2005, and correspond to their values in the Dow Jones and London Metals Exchange markets. The graph must be understood as an orientative tool more than a source of quantitative data. Group A corresponds to low cost materials, which are used in common mass applications for industry: iron, steels, some master alloys, magnesium and aluminium. This group seems to be the one from which alloying elements should be selected for low cost development, as their price is lower than the Ti price. Group B includes medium and high cost materials, which are used less in mass industry, including titanium, vanadium, nickel and cobalt. Group C includes very high cost materials, even more expensive than Ti, so their introduction as alloying elements would increase the cost of the final material.

The selection of alloying elements must meet some requirements to avoid undesired effects. One limitation is the possible formation of intermetallics in the microstructure, which could cause embrittlement of the material. There are only a few beta stabilisers that do not form intermetallics with Ti. These elements are described as isomorphous and include Mo, V, Ta and Nb. Unfortunately, these elements belong to the high cost and very high cost groups of materials, so their use increases the price of the alloy composition. The other beta stabilisers are named 'eutectoids', and form intermetallic compounds with Ti, so their use has been avoided in materials for the aerospace industry.

Some examples of 'eutectoid' beta stabilisers are Mn, Fe, Cr, Co, Ni, Cu and Si. Most of these elements belong to the low cost group, so they are good candidates as alloying elements provided that the formation of intermetallics is avoided. Some of these elements present very sluggish eutectoid decompositions, so the formation of intermetallic phases can be controlled during manufacture or service of the materials. Fe has been reported to have a slow intermetallic formation,[15] so its use is feasible since intermetallic formation can be avoided. In the Ti–Fe phase diagram shown in Fig. 2,[16] it is clear that intermetallic TiFe is thermodynamically stable at room temperature for a wide range of alloy compositions. Despite this known stability, there are currently commercial alloys containing Fe as an alloying element, i.e. TIMETAL low cost beta (LCB, Ti–1·5Al–5·5Fe–6·8Mo) and Ti–5Al–2·5Fe. From this approach, LCB takes advantage of the use of master alloys commonly used for the manufacturing of steels, which lowers the cost of the alloy composition. Among the limitations of the use of Fe in Ti alloys are the segregations that can occur during ingot metallurgy processes due to the different densities of the metals. Such a problem is avoided with the use of conventional PM techniques.

Ti–Fe alloys have been the subject of previous studies, with most of them focused on cast alloys, including studies of the mechanical oxidation of the alloys,[17] heat treatment response[18,19] or their structure and properties.[20]

Regarding the PM route, there are some reports on Ti–Fe alloys. Among them, the effect of Fe on the sintering behaviour of Ti was studied by Wei *et al.*,[21] who reported the enhancement of the sinterability of Ti alloys by the addition of 5 wt-%Fe. No liquid phase formation was found during sintering due to the fast solid state diffusion of Fe in Ti. Wei *et al.* suggested the use of coarser particles and higher heating rates to make use of the positive effect of Fe on the initial sintering stage of Ti. In the present work, the comparison among fine and coarse Fe particles is discussed.

Powders to be used as alloying elements for Ti must be studied to evaluate the feasibility of different powder grades, the influence of particle size, morphology, purity, etc. One more consideration to take into account is that master alloys, which are used for Fe formulation, frequently present impurities that make them unsuitable for Ti alloying, as they diminish its mechanical properties. Thus, the use of a master alloy is conditional on its purity, and the use of elemental Fe could be preferred since it permits better control over the purity of the powders in order to avoid undesired contamination of the alloys. The PM industry produces iron powder as a

Table 2 Studied materials.

	Materials
Base material	Ti
Ti–7Fe alloys	Ti–7Fe(ASC100·29)
	Ti–7Fe(carbonyl)
	Ti–7Fe(Fe–25Ti)

Table 1 Characteristics of starting powders.

	Type	Powder	O, wt-%	N, wt-%	Purity, %	Supplier	Mean particle size, μm	D_{10}, μm	D_{50}, μm	D_{90}, μm
Ti base powder	Ti elemental	Ti(HDH)	0·319	0·008	99·6	GfE	54	24	51	88
Fe additions	Fe elemental	Fe ASC100·29	0·094	0·003	99·9	Höganäs	97	38	88	169
		Fe carbonyl	0·244	0·007	…	ECKA	8	3	7	14
	Master alloy	Fe–25Ti	1·91	0·50	91·5	LSM	25	6	22	46

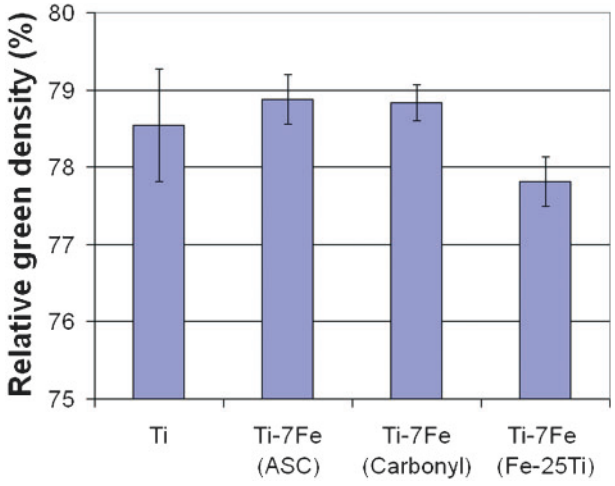

3 Relative green density for samples pressed at 500 MPa

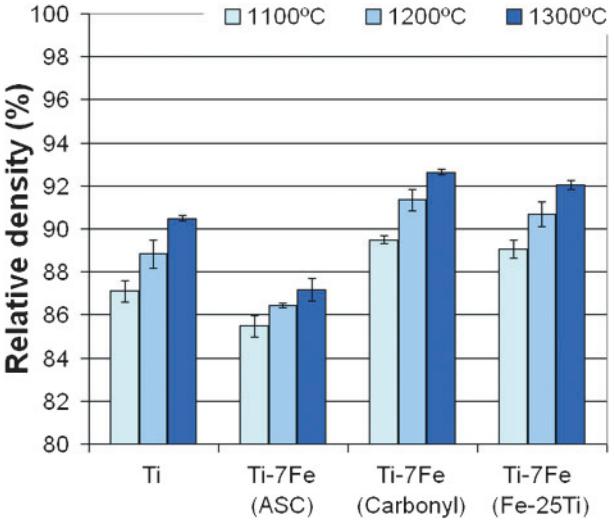

4 Relative density values for materials sintered at different temperatures

commodity, so the cost of commercial powder is optimised, and the quality and purity of Fe are suitable for addition to titanium for alloying.

Regarding Ti powders, the variety of types available opens up different possibilities. One of the common assertions that can be made for all of the powders is that a higher purity and compressibility results in better mechanical properties of the final materials. In previous developments, the sponge Ti powder was known to contain chlorides that hindered the full densification of parts, even after hot isostatic pressing. Hydride–dehydride Ti powders are chloride free, and have high purity at a reasonable cost.[22] The development of low cost Ti alloys needs revision of these concepts, and selection of the proper low cost powder will be the key parameter to success. The conventional PM processing (pressing + sintering) requires high compressibility powders to attain good dimensional tolerances and avoid the post-processing of sintered parts. Currently, there is no commercial Ti powder optimised for being pressed. The influence of the purity of Ti powders on compaction is to be published elsewhere. More research must be carried out in order to develop Ti powders optimised for processing by conventional PM techniques.

In the present work, the effects of different Fe powder additions on the sinterability of Ti–Fe alloys are discussed. Properties and microstructure features of sintered parts are discussed for the β-Ti–7Fe alloys.

Experimental procedure

Alloys with the composition Ti–7Fe were manufactured by blending elemental Ti with three different powder additions containing Fe. Two elemental powder additions and a master alloy were used. Some characteristics of the powders are summarised in Table 1.

Table 2 shows the different materials prepared for this study, divided into the non-alloyed base material Ti(HDH) and Ti–7Fe alloys.

Powders were blended in a Turbula mixer for 1 h, and tensile specimens were uniaxially pressed at 500 MPa to make the flat geometry specified in the standard MPIF 10.[23] Sintering was carried out in a high vacuum tubular furnace at 2×10^{-5} mbar at temperatures ranging from 900 to 1300°C for 1 h, with heating and cooling rates of 5°C min^{-1}. Sintering substrates were made from full dense ZrO_2 granules with diameters ranging from 1·9 to 2·5 mm, commercialised as Zirmil by Saint-Gobain (France).

Green densities were calculated from the dimensions of the samples. The density of sintered samples was measured by the Archimedes method. Theoretical densities of the blends were calculated using the mixing rule.

Hardness HV30 was measured in a Vickers hardness tester Gnehm OM-150. Tensile strength tests were carried out following the EN10002-1:2001 standard,[24] with a displacement rate of 1 mm min^{-1} using load cells of 50 kN, and an extensometer with an initial length of 22·2 mm. The average section of the samples was 31 ± 2 mm^2, and no variation of the area was considered during the tests for the calculations. Microstructure and fracture surface analysis were performed by SEM. Microstructures of materials sintered at 1300°C are presented after etching with a solution containing 4 vol.-%HF.

Differential thermal analysis (DTA) was performed in Setsys Evolution 16/18 equipment from Setaram Instrumentation. The experiments were carried out in argon at temperatures up to 1350°C at a heating rate of 5°C min^{-1} in ZrO_2 crucibles. Powder samples were weighted at 60 mg and were previously pressed at 500 MPa to maintain the same particle contacts as in sintering conditions. The reference crucible was empty. Oxygen and nitrogen analysis were performed in Leco TC-500 equipment using the ASTM standards for measuring these interstitials on Ti.[25,26]

X-ray diffraction analysis was carried out in a Philips X'Pert with Cu K_α radiation, covering an angle 2θ from 20 to 120°, performed on sections of the samples.

Results and discussion

Pressing and sintering

One of the most important aspects to consider in the PM process is the achievement of high green density values after pressing. The higher the green density, the lower the dimensional change that the parts will suffer during sintering, which is a basic condition for maintaining

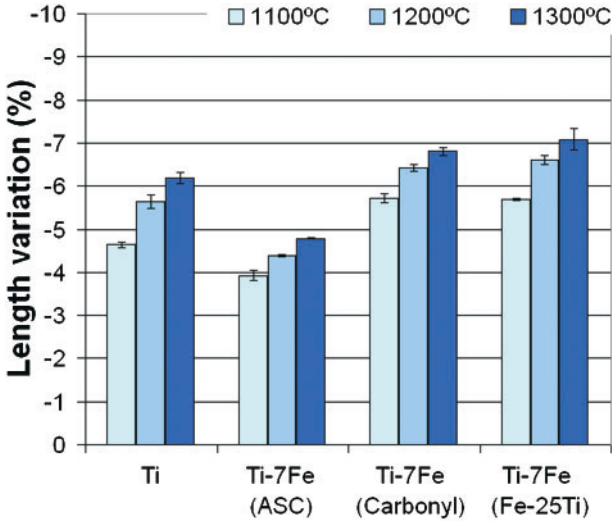

5 Length variation for materials sintered at different temperatures

dimensional tolerances and avoiding costly finishing operations.

Relative green density values obtained for the different blends pressed at 500 MPa are shown in Fig. 3. All the density values were similar and lower than expected, although the blends with Fe carbonyl and Fe ASC100·29 achieved the highest values. Fe–25Ti additions diminished the compressibility of the blend with respect to the base powder.

The available commercial Ti powders are not optimised for pressing at the present time. Additionally, the purity of Ti plays a very important role, as interstitial impurities in solid solution strengthen Ti and make the plastic deformation of the powders more difficult. Regarding the physical properties of Ti, the hcp lattice structure of pure titanium, in conjunction with its low modulus, endows the material with a high resilience, which hinders plastic deformation during pressing. However, the high reactivity of Ti gives it poor tribological properties, which leads to the development of high friction forces of the powders with the die walls in comparison with commercial, pure Fe powders, which results in losses in pressing efficiency.[27–29] The addition of Fe powder slightly improves this behaviour.

The relative densities of sintered materials are represented in Fig. 4. The values ranged from 86 to 93% of the theoretical densities, increasing with the sintering temperature in all cases. The highest values were obtained in materials blended with Fe carbonyl, while the lowest densities were reached by materials alloyed with Fe ASC100·29, whose values were even lower than those obtained for the Ti base powder.

It should be pointed out that the main difference between Fe carbonyl and Fe ASC100·29 powders is related to their particle size. Fe carbonyl and Fe–25Ti powders present a markedly smaller particle size

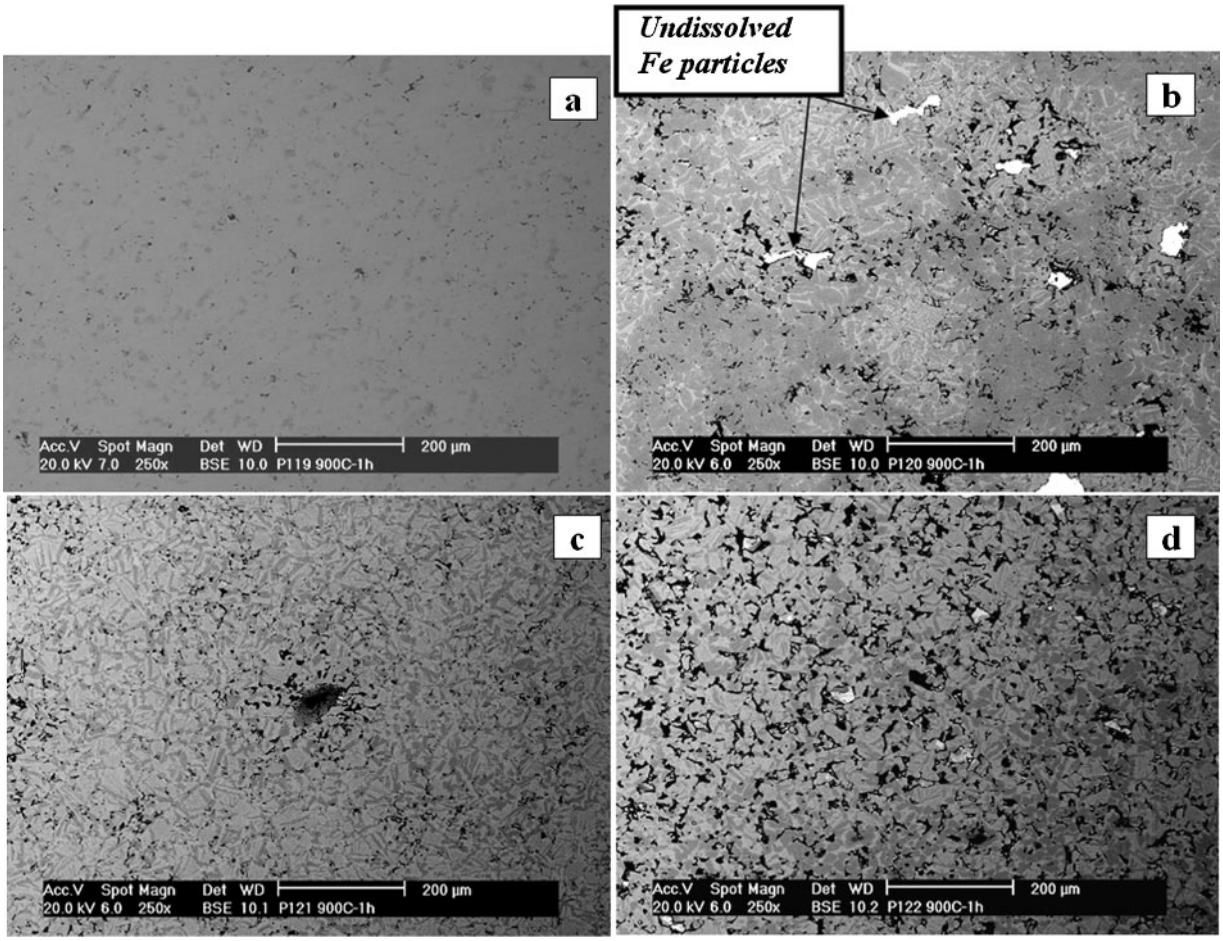

a Ti; *b* Ti–7Fe(ASC); *c* Ti–7Fe(carbonyl); *d* Ti–7Fe(Fe–25Ti)

6 Scanning electron microscopy images (BSE mode) of microstructures of materials sintered at 900°C for 1 h at 5°C min^{-1}

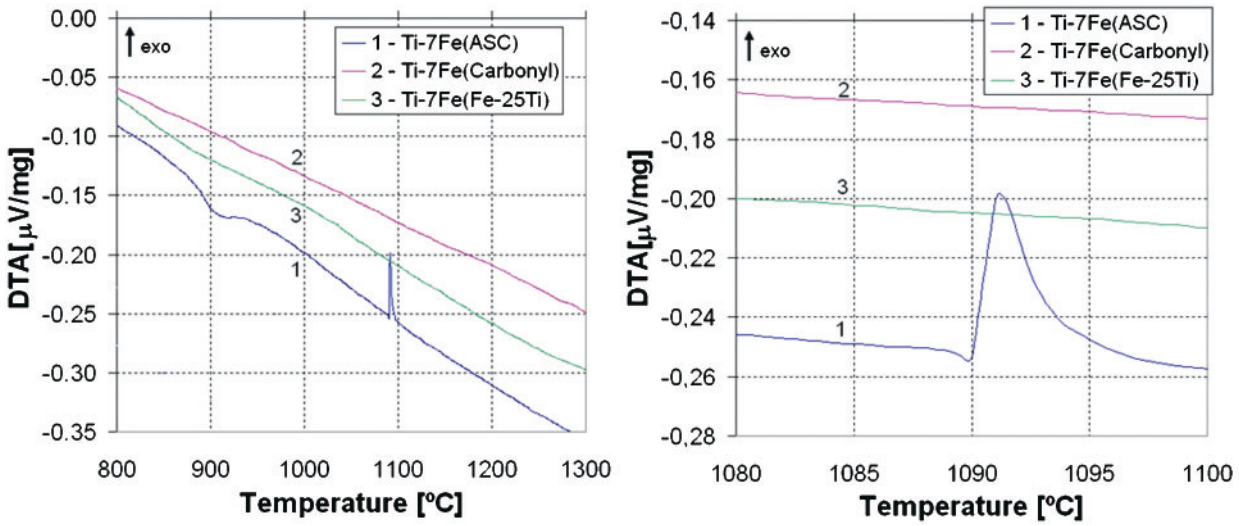

7 Analysis (DTA) for Ti–7Fe samples at heating and cooling rates of 5°C min^{-1}: right image shows detail of exothermic reaction

compared to that of the Fe ASC100·29. This is also noticeable if the relative density of the alloys is compared to the relative density of unalloyed Ti, which reveals that Fe carbonyl and Fe–25Ti promote sintering, whereas Fe ASC100·29 hinders Ti densification.

Important dimensional changes were observed in all materials after sintering. The length variation for the materials sintered at different temperatures is represented in Fig. 5. As shown above for density, dimensional change followed the same trend, increasing with the sintering temperature, and achieving shrinkage values of $\sim$7% for the highest temperature studied.

Differences in the particle size of Fe additions led to different sintering mechanisms, either conventional solid state sintering or reactive sintering. Fe ASC100·29 powder, with a large particle size, caused residual porosity due to two effects:

(i) the formation of large pores promoted by the exothermic reaction between Ti and Fe
(ii) Kirkendall porosity due to the asymmetric diffusion between Fe and Ti.

Fe atoms diffuse much faster into Ti particles than Ti atoms into Fe particles, with diffusion coefficients that differ by more than two orders of magnitude.[30–32] To illustrate this behaviour, Fig. 6 shows the microstructures of the base Ti and the three Ti–7Fe alloys, all sintered at 900°C for 1 h. This low sintering temperature was intentionally selected below the eutectic point (1085°C) to analyse the sintering mechanisms. Figure 6*a* shows an image of the base material, which basically consists of α-Ti with pores in the microstructure. Figure 6*b* corresponds to a material obtained with Fe ASC100·29 powder, where Fe particles can be identified by the bright contrast areas. With a heating rate of 5°C min^{-1} and a dwell time of 1 h at 900°C, coarse Fe particles did not diffuse completely into Ti. Figure 6*c* shows the material obtained with Fe carbonyl, with no evidence of elemental Fe particles, which diffused completely at 900°C. The same result was reported by Wei *et al.*[21] for Ti–5Fe alloys using Fe particles with a mean size of 19 μm. Figure 6*d* shows the microstructure of the material obtained with master alloy Fe–25Ti, showing that few particles remained in the microstructure at 900°C.

The thermal analysis curves presented in Fig. 7 illustrate the consequences of these different diffusion stages depending on the Fe addition. The DTA curve for the blend Ti–7Fe(ASC) shows an exothermic reaction at 1090°C. This reaction corresponds to a self-propagated reaction, reported by some authors as liquid phase formation in the periphery of Fe particles that promotes the local exothermic reaction of Ti and Fe to form intermetallic TiFe.[33] In the right graph, the detail of the exothermic reaction in the Ti 7Fe(ASC) DTA shows an endothermic transformation at the beginning of the peak, which could imply liquid phase formation. Since the eutectic liquid that forms has solubility in Ti, the liquid phase is transient,[34] so sintering is temporarily governed by this phase. Transient liquid phase sintering in the Fe–Ti system has been studied by other authors in reports related to steel with Ti additions,[35,36] in which Ti was the minority element and where solid diffusion of Ti into Fe was too slow to complete Ti dissolution, leading to melting of the Ti particles. Some of these reports indicated swelling of the samples at the eutectic temperature (1085°C) when using elemental powder mixtures. Benefits in sintering were reported if the eutectic reaction of Ti–Fe is avoided by the use of intermetallic additions (Fe–25Ti) instead of elemental additions, promoting sintering with the Fe-rich eutectic liquid phase (1289°C).[37]

The DTA curves show that Fe carbonyl and Fe–25Ti additions do not promote reactions during sintering, leading to a solid state sintering mechanism in both cases. The absence of transformations in their DTA curves indicates that the diffusion of Fe carbonyl is completed below 1085°C, and diffusion of Fe–25Ti is completed below 1289°C (see phase diagram in Fig. 2). The curves are coherent with the microstructures observed by SEM.

The lower rate of dissolution of Fe ASC100·29 particles can be noticed by analysing its DTA curve, where an endothermic transformation is identified at 882°C, which, in fact, corresponds to the α–β transformation temperature of pure Ti. This evidence indicates that a high amount of elemental Ti remained unchanged in the blend with Fe ASC100·29 at this temperature, while the blends with Fe carbonyl and Fe–25Ti did not

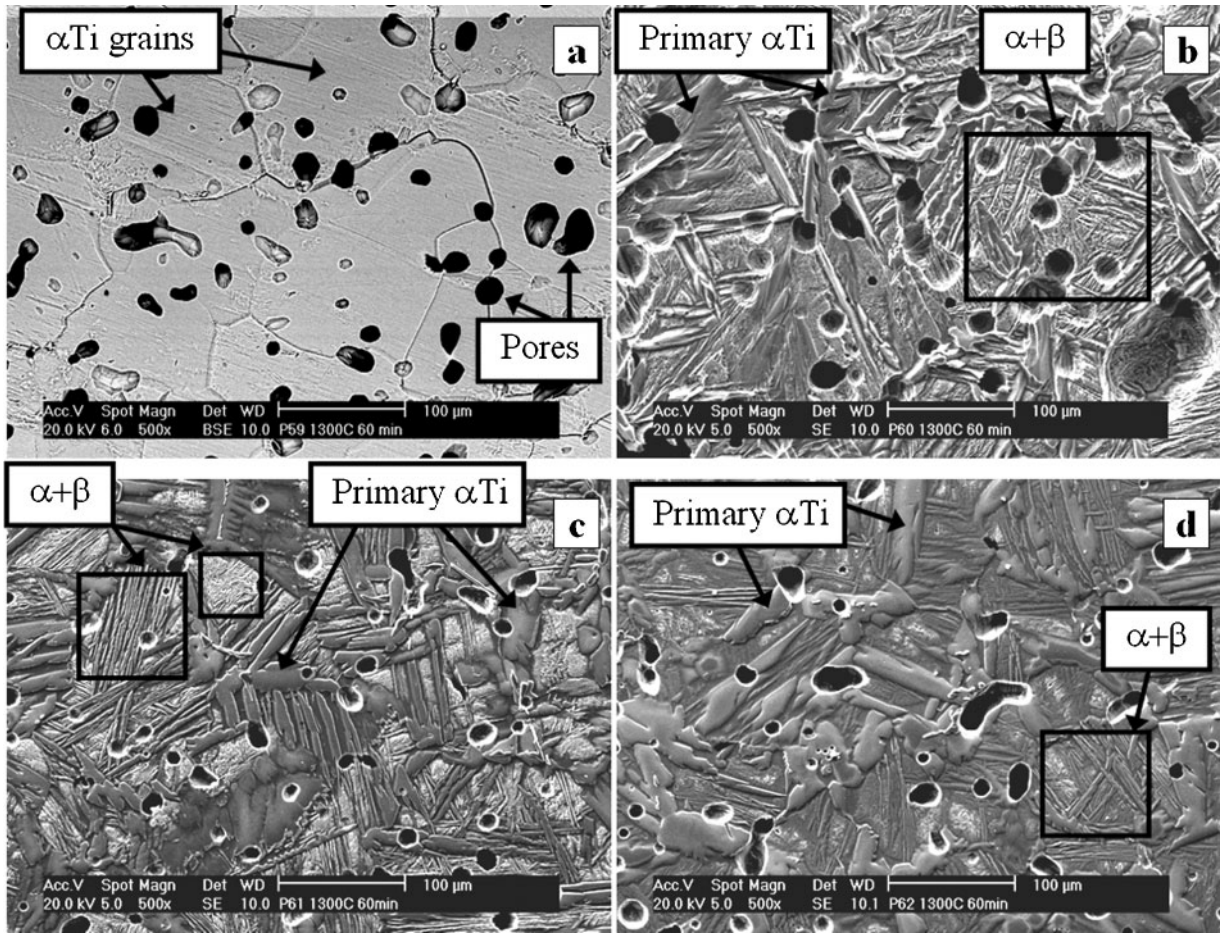

a Ti; *b* Ti–7Fe(ASC); *c* Ti–7Fe(carbonyl); *d* Ti–7Fe(Fe–25Ti)

8 Images (SEM) of materials sintered at 1300°C for 1 h at 5°C min^{-1}

show this endothermic transformation, demonstrating that little or no elemental Ti remained in their microstructures at 882°C, and that the allotropic transformation from α to β was completed by the diffusion of Fe into the Ti lattice during heating of the samples. For the Fe carbonyl and Fe–25Ti blends, DTA curves showed a slight sign of transformation at temperatures between 550 and 600°C that were close to the eutectoid transformation temperature (595°C). The allotropic transformation of α–β seems to start at this temperature, and continues during the heating of the samples.

At higher sintering temperatures, different microstructures were developed depending on the Fe addition type. Scanning electron microscope images of Ti and Ti–7Fe microstructures sintered at 1300°C for 1 h are shown in Fig. 8. Figure 8*a* shows the microstructure of the base powder Ti, and Fig. 8*b* shows the material

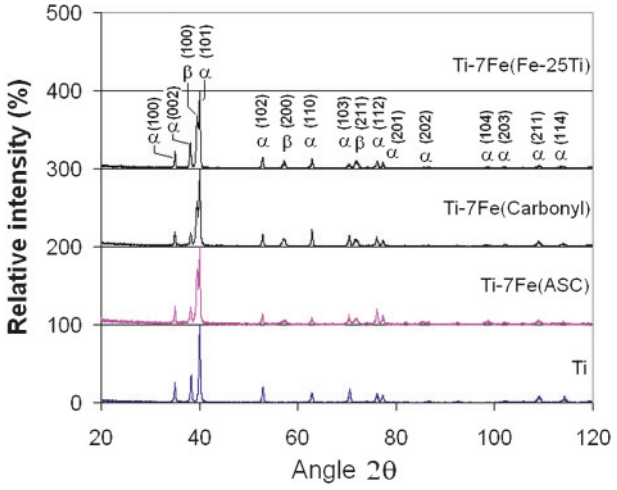

9 Analysis (XRD) of materials sintered at 1300°C for 1 h at 5°C min^{-1}

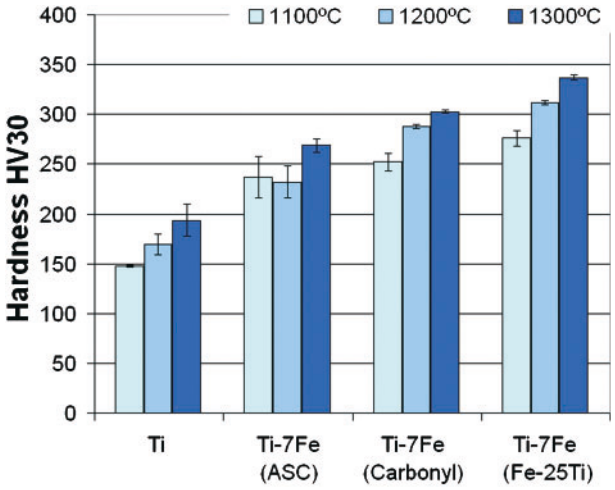

10 Vickers hardness values for all materials sintered at different temperatures for 1 h

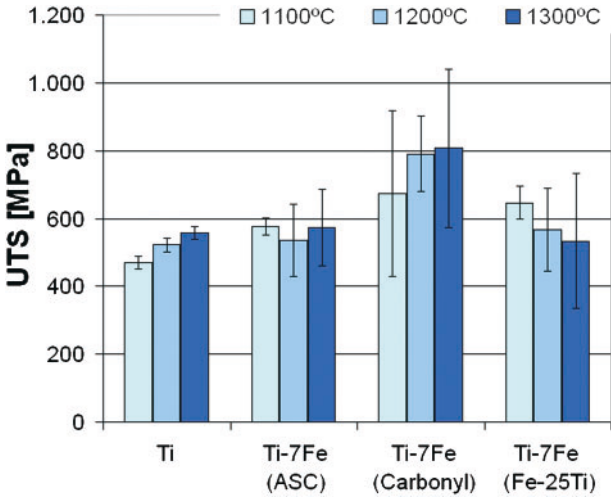

11 Tensile strength of materials sintered at different temperatures

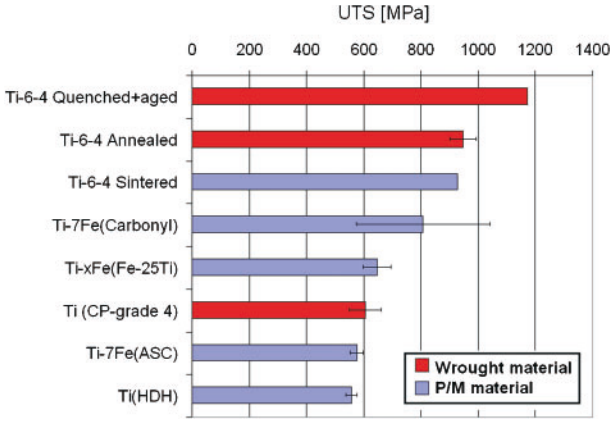

12 Tensile strength of studied materials compared to conventional Ti alloys[38,39]

blended with Fe ASC100·29 powder, with a pore size much higher than those developed in materials blended with Fe carbonyl (Fig. 8*c*) and master alloy Fe–25Ti (Fig. 8*d*). It can be asserted that additions of coarse Fe powder lead to the formation of large pores. The lower quantity and smaller size of the porosity present in the materials obtained with blends from Fe carbonyl and master alloy Fe–25Ti are similar to those of the base material Ti.

The microstructures of materials 'as sintered' are bimodal, formed by primary alpha phase and secondary alpha phase in the form of fine lamellae. Beta phase is retained between the alpha lamellae. The composition of the microstructures differs from the data obtained in the equilibrium phase diagram shown in Fig. 2. The XRD analysis of the sintered materials (Fig. 9) showed that only alpha and beta phases were present in the microstructures, and no trace of intermetallics TiFe or $TiFe_2$ were found in the processing conditions.

Mechanical properties

Regarding the hardness of materials, a clear increase with the sintering temperature can be observed in all materials (Fig. 10), following the same trend as density. Hardness values were higher for the alloys than for the base material, as was expected due to the solid solution strengthening and to the bimodal microstructures found in the alloys. Hardness values of the alloys were higher, even in the cases where the alloys presented lower sintered density than the base material.

Among the alloys, those made from Fe carbonyl showed higher hardness values than those from Fe ASC100·29, thanks to the higher density achieved in materials made with Fe carbonyl. However, the highest hardness values were obtained in materials produced from Fe–25Ti master alloy, and were higher than those found for materials produced from Fe carbonyl, despite its lower density. The reason could be related to the impurities contained in the master alloy, which are dissolved in Ti during the sintering step, hardening the final material by solid solution. These impurities include O, N, Al, Si and V. The oxygen and nitrogen contents of materials sintered at 1200°C for 1 h are presented in Table 3, where it is clearly shown that Fe–25Ti has introduced high amounts of interstitials into the materials.

Table 3 Oxygen and nitrogen contents in samples sintered at 1200°C

	O, wt-%	N, wt-%
Ti	0·35±0·02	0·015±0·001
Ti–7Fe(ASC)	0·34±0·01	0·013±0·002
Ti–7Fe(carbonyl)	0·34±0·02	0·013±0·003
Ti–7Fe(Fe–25Ti)	0·53±0·04	0·10±0·01

Tensile strength did not follow the same clear tendency as the hardness–temperature–density relationship. Figure 11 shows that the tensile strength of the different groups of materials did not vary at the three temperatures tested. The relatively constant values of the tensile strength with the sintering temperature could be related to the pore size of the remaining porosity. The high scattering of the UTS values suggested the effects of large defects, which enhance the impact of the low ductility of the materials. Even with the highest densities, there could be internal and surface defects over a critical size that could concentrate sufficient stress to diminish the strength of the alloys. Additionally, grain growth occurs when sintering temperatures are increased, so the benefits of smaller pores and lower porosity could be balanced with a higher grain size.

It is worth comparing these results with the UTS of the commercial reference alloy Ti–6Al–4V. Figure 12 compiles data from different sources,[38,39] showing that the alloys from Fe carbonyl studied in the present work attained tensile strength mean values higher than 800 MPa, and maximum values near 1000 MPa, which are comparable to the values for the conventional wrought Ti–6Al–4V (900 MPa). It should also be pointed out that sintered Ti showed similar tensile strength to wrought 'ASTM CP-Ti grade 4'.

The strength of the alloys produced from Fe–25Ti was lower than expected from the results shown above for density and hardness. This behaviour seems to be related to the combined effects of residual porosity and the presence of impurities in the master alloy that over-hardens the material, making the material more brittle. The effects of impurities from Fe–25Ti(N,O,Al) seem to decrease the fracture toughness of the materials. This fact seems to be supported by the large brittle areas found in the fracture surface of materials made from Fe–25Ti (Fig. 13).

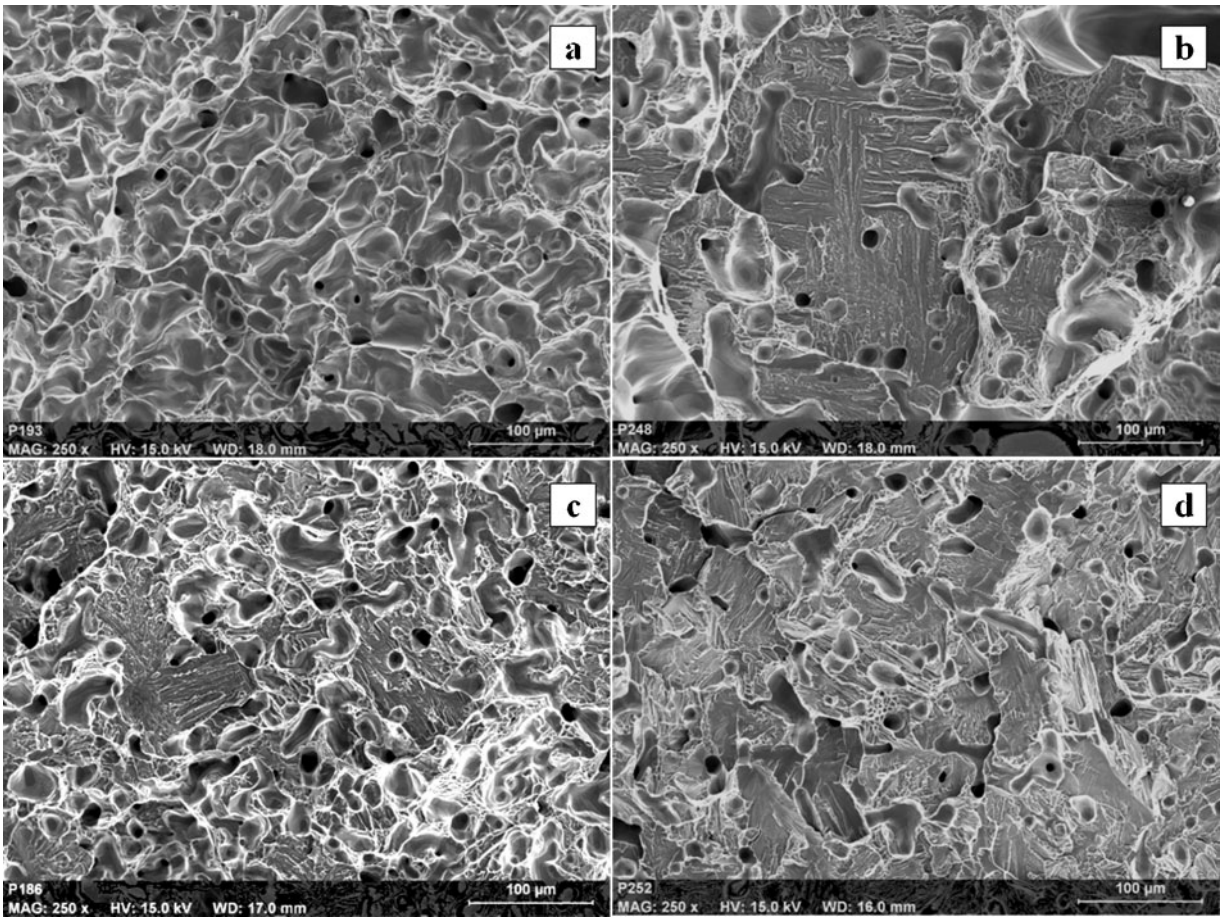

a Ti; *b* Ti–7Fe(ASC); *c* Ti–7Fe(carbonyl); *d* Ti–7Fe(Fe–25Ti)

13 Fracture surface of Ti–7Fe materials

Despite the promising values of UTS, the elongation of the materials was low, typical for sintered materials processed by the low cost conventional powder metallurgy route of pressing and sintering, where finishing processes to close residual porosity have not been carried out. The elongation values obtained by the different materials (Fig. 14) were 6% for the base material, and in between 1 and 2% for the alloys. Among Ti–7Fe materials, the highest values were attained with those made from Fe carbonyl.

The stress–strain curves obtained for the best material in each family are represented in Fig. 15. The curve obtained for pure Ti presented a clear plastic deformation, with a yield strength of 400 MPa, reaching an UTS near 600 MPa at 14% of maximum deformation. The alloys presented different behaviours, especially the alloys made from Fe ASC100·29 and Fe–25Ti, where the rupture was not preceded by a plastic deformation stage. The material made from Fe carbonyl presented plastic deformation, but deformation at fracture was

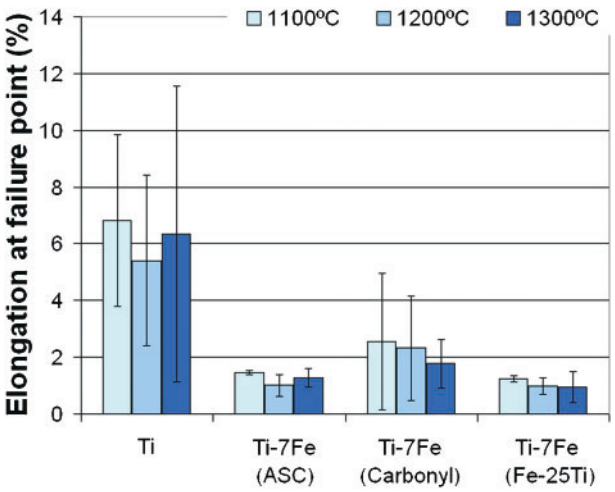

14 Elongation for materials sintered at different temperatures

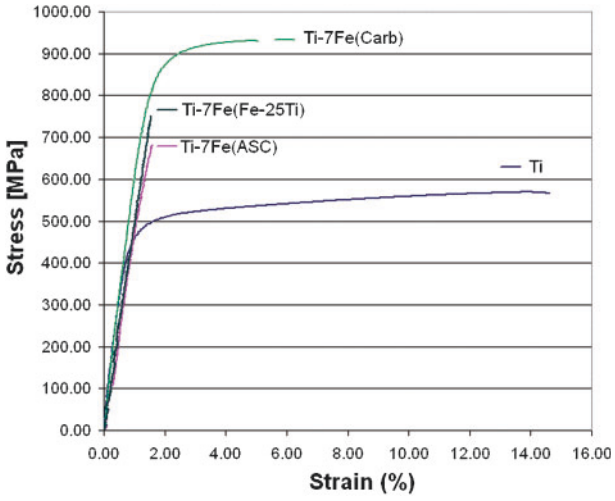

15 Selection of stress–strain curves for different families of materials

lower than 6%. Among all of the studied materials, pure Ti showed the highest elongation values, although the deviation of the measurements was very high.

The scattering in strength and elongation was high for all of the families, especially in deformation values. The optimisation of the process can contribute to more reproducible results. In particular, a better understanding of the pressing step could stabilise material properties, thereby obtaining high density materials from the very first stage of the powder metallurgy process. Powder homogeneity and purity are also key parameters for the achievement of high green densities. Impurities, present in the base powder and in the alloying elements, harden and embrittle sintered materials, reducing their strength and ductility.

It should be noted that mechanical properties of the Ti–7Fe alloys are strongly dependent on the type of Fe addition, yielding different final microstructures in terms of quantity, distribution, morphology and size of porosity. As shown in Fig. 8, Fe ASC100·29 led to coarse residual porosity. Fe carbonyl and Fe–25Ti master alloy powders presented smaller particle sizes and consequently, led to a finer residual porosity. However, for both of the latter families, despite the similar residual porosity, the mechanical and fracture behaviours were quite different.

Primary alpha phase is ductile with respect to the secondary alpha and beta phases, which can be noticed in the fracture surfaces shown in Fig. 13. Figure 13*a* presents the fracture surface of the Ti base material, showing the typical fracture topography of a ductile material where plastic deformation has taken place. This behaviour is characteristic of pure Ti, completely formed by unalloyed alpha phase. The fracture surfaces of pure Ti were different from those obtained for Ti–7Fe alloys, which presented areas of brittle fracture and some areas of ductile fracture, depending on the material. An example of the fracture surfaces obtained in the materials produced from Fe ASC100·29 is shown in Fig. 13*b*, where a large zone of cleavage, characteristic of a fragile behaviour, can be perfectly appreciated.

The fracture surfaces obtained for the samples made from Fe carbonyl (Fig. 13*c*) showed brittle cleavage areas, but also ductile areas similar to those observed for the base material (Ti). Those areas are probably responsible for the initial plastic behaviour before the rupture shown in the stress–strain curves of this family of alloys (Fig. 15).

Alloys made from Fe–25Ti showed more numerous brittle areas. Since porosity was similar to alloys made from Fe carbonyl, the embrittlement seems to be associated with the solid solution strengthening of the primary alpha phase by the impurities contained in the master alloy, which could diminish fracture toughness.

Conclusions

Ti–7Fe alloys were prepared from different Fe powders by blending. Although the elemental Fe additions slightly improved the compressibility of the base material, the green densities were low in all cases (78–79%), probably due to the poor compressibility of Ti powders. The blend made with Fe–25Ti additions had lower compressibility than the base powder. Sintered materials reached density values of up to 93% of the theoretical density in materials made with Fe carbonyl, leading to high dimensional changes in all cases (around 7%). The introduction of coarse Fe ASC100·29 particles led to microstructures with large pores, probably caused by the combined effects of the coalescence of Kirkendall pores and reactive sintering, which probably led to transient liquid phase formation.

Master alloy Fe–25Ti completed diffusion at higher temperatures than Fe carbonyl, but no evidence of liquid phase formation was found in blends carried out with these additions. Sintering occurred in the solid state in both cases, and similar residual pore sizes were found with these additions.

Hardness was found to be dependent on the porosity, as well as on the composition of the materials. The lowest hardness value was found for pure Ti (200 HV30), while the highest values were found for alloys made from Fe–25Ti (330 HV30), due to the solid solution strengthening caused by the impurities contained in the master alloy.

The highest strength was attained with materials made from Fe carbonyl, which reached UTS values around 800 MPa, comparable to conventional Ti–6Al–4V wrought alloy. Additions of Fe ASC100·29 and the master alloy Fe–25Ti used in this study have proven to not be efficient at enhancing the mechanical properties of the Ti base material.

Acknowledgements

The authors would like to acknowledge financial support from the Comunidad de Madrid to carry out this research through the programme ESTRUMAT-CM (reference MAT/77), and from the Ministry of Education through the R&D Project MAT2006-02458.

References

1. M. J. Donachie: 'Titanium: a technical guide'; 1988, Materials Park, OH, ASM International.
2. G. Lütjering and J. C. Williams: 'Titanium (engineering materials and processes)'; 2003, Berlin, Springer-Verlag.
3. EHKTechnologies: 'Opportunities for low cost titanium in reduced fuel consumption, improved emissions, and enhanced durability heavy-duty vehicles', Subcontract 4000013062, EHKTechnologies, Vancouver, WA, USA, 2002.
4. C. A. Lavender: 'Low-cost titanium evaluation', Pacific Northwest National Laboratory, Richland, WA, USA, 2004.
5. EHKTechnologies: 'Summary of emerging titanium cost reduction technologies. A study performed for US Department of Energy and Oak Ridge National Laboratory', Subcontract 4000023694, EHKTechnologies, Vancouver, WA, USA, 2004.
6. G. Crowley: 'How to extract low-cost titanium', *Adv. Mater. Processes*, 2003, **161**, (11), 25–27.
7. G. Z. Chen, D. J. Fray and T. W. Farthing: 'Direct electrochemical reduction of titanium dioxide to titanium in molten calcium chloride', *Nature*, 2000, **407**, 361–364.
8. F. H. Froes and D. Eylon: 'Powder-metallurgy of titanium-alloys', *Int. Mater. Rev.*, 1990, **35**, (3), 162–182.
9. J. E. Smugeresky and D. B. Dawson: 'New titanium alloys for blended elemental powder processing', *Powder Technol.*, 1981, **30**, (1), 87–94.
10. T. Fujita, A. Ogawa, C. Ouchi and H. Tajima: 'Microstructure and properties of titanium alloy produced in the newly developed blended elemental powder metallurgy process', *Mater. Sci. Eng. A*, 1996, **A213**, (1–2), 148–153.
11. 'Recent developments in PM of titanium', *Met. Powder Rep.*, 2002, **57**, (10), 46.
12. M. Hagiwara and S. Emura: 'Blended elemental P/M synthesis and property evaluation of Ti-1100 alloy', *Mater. Sci. Eng. A*, 2003, **A352**, (1–2), 85–92.
13. O. M. Ivasishin: 'Cost-effective manufacturing of titanium parts with powder metallurgy approach', *Mater. Forum*, 2005, **29**, 1–8.

14. Y. Liu, L. F. Chen, H. P. Tang, C. T. Liu, B. Liu and B. Y. Huang: 'Design of powder metallurgy titanium alloys and composites', *Mater. Sci. Eng. A*, 2006, **A418**, (1–2), 25–35.
15. R. I. Jaffee: 'The physical metallurgy of titanium alloys', *Prog. Met. Phys.*, 1958, **7**, 65–163.
16. J. L. Murray: 'Phase diagrams of binary titanium alloys'; 1987, Materials Park, OH, ASM International.
17. D. B. Lee, K. B. Park, H. W. Jeong and S. E. Kim: 'Mechanical and oxidation properties of Ti–*x*Fe–*y*Si alloys', *Mater. Sci. Eng. A*, 2002, **A328**, (1–2), 161–168.
18. F. C. Holden, H. R. Ogden and R. I. Jaffee: 'Heat treatment and mechanical properties of Ti–Fe alloys', *Trans. Am. Inst. Min. Metall. Eng.*, 1956, **206**, (5), 521–528.
19. K. Majima, T. Isono and K. Shouji: 'Effect of heat treatment on the sintered Ti–Fe alloys', in Proc. Conf. Sintering '87, Vol. 1, 599–604; 1987, New York, Elsevier.
20. D. J. Lin, C. P. Ju and J. H. C. Lin: 'Structure and properties of cast Ti–Fe alloys', *Trans. Am. Foundry. Soc.*, 1999, **107**, 859–864.
21. W. Wei, Y. Liu, K. Zhou and B. Huang: 'Effect of Fe addition on sintering behaviour of titanium powder', *Powder Metall.*, 2003, **46**, (3), 246–250.
22. E. Fukasawa, R. Murayama and W. Kagohashi: 'Characteristics of high-purity titanium powder by HDH process', in Proc. Conf. Titanium '92: Science and Technology, (ed. F. H. Froes *et al.*), Vols. 1–3, 919–926; 1993, Warrendale, PA, TMS.
23. 'Tension test specimens for pressed and sintered metal powders', MPIF Standard 10, Metal Powder Industries Federation, Princeton, NJ, USA, 1963.
24. 'Tensile testing of metallic materials. Method of test at ambient temperature', UNE EN10002-1:2001, AENOR, Madrid, Spain, 2001.
25. 'Standard test method for determination of oxygen and nitrogen in titanium and titanium alloys by the inert gas fusion technique', E-1409, ASTM, Philadelphia, PA, USA, 2005.
26. 'Standard test method for determination of nitrogen in titanium and titanium alloys by the inert gas fusion technique', E-1937, ASTM, Philadelphia, PA, USA, 2004.
27. Y. Hovanski, C. A. Lavender and K. S. Weil: 'Evaluation of the pressing characteristics of commercially pure titanium using an instrumented double acting die', Proc. 2008 World Cong. on 'Powder metallurgy and particulate materials', Washington, DC, USA, June 2008, MPIF.
28. S.-T. Hong, Y. Hovanski, C. A. Lavender and K. S. Weil: 'Investigation of die stress profiles during powder compaction using instrumented die', *J. Mater. Eng. Perform.*, 2008, **13**, (3), 382–386.
29. A. Simchi and G. Veltl: 'Behaviour of metal powders during cold and warm compaction', *Powder Metall.*, 2006, **49**, (3), 281–287.
30. H. Nakajima, K. Yusa and Y. Kondo: 'Diffusion of iron in a diluted α-Ti–Fe alloy', *Scr. Mater.*, 1996, **34**, (2), 249–253.
31. H. Nakajima, S. Ohshida, K. Nonaka, Y. Yoshida and F. E. Fujita: 'Diffusion of iron in *β*-Ti–Fe alloys', *Scr. Mater.*, 1996, **34**, (6), 949–953.
32. B. Kieback and W. Schatt: 'Anwendung eines kurzzeitigen Flüssigphasensinterns für die Herstellung von Fe–Ti-Sinterlegierungen', *Planseeber. Pulvermet.*, 1980, **28**, 204–215.
33. C. S. Wang, K. S. Zhang, H. J. Pang, Y. Z. Chen and C. Dong: 'Laser-induced self-propagating reaction synthesis of Ti–Fe alloys', *J. Mater. Sci.*, 2008, **43**, 218–221.
34. R. M. German: 'Liquid phase sintering'; 1985, New York, Plenum Press.
35. B. F. Kieback, W. Schatt and E. Friedrich: 'Sintering of titanium alloyed steels', *Powder Metall.*, 1985, **28**, (2), 93–96.
36. B. F. Kieback, W. Schatt and G. Jangg: 'Titanium-alloyed sintered steels', *Powder Metall. Int.*, 1984, **16**, (5), 207–212.
37. W. H. Baek and R. M. German: 'Transient liquid-phase sintering in the Fe–Fe_2Ti system', *Int. J. Powder Metall.*, 1986, **22**, (4), 235–244.
38. 'Guide to engineered materials (GEM2002)', *Adv. Mater. Processes*, 2001, **159**, (12), 29–184.
39. F. H. Froes and D. Eylon: 'Powder-metallurgy of titanium-alloys – a review', *Powder Metall. Int.*, 1985, **17**, (4), 163–167.